Catalysis Science & Technology

ROYAL SOCIETY OF CHEMISTRY

PAPER

View Article Online
View Journal

Cite this: DOI: 10.1039/d4cy01192a

Controlling the reactivity of enol ether radical cations *via* the substitution pattern: investigation into electrochemically induced Diels–Alder reactions†

Haruka Morizumi,[a] Yanan Han,[b] Olga S. Bokareva,[bc] Robert Francke,*[b] Yoshikazu Kitano[a] and Yohei Okada*[a]

Received 7th October 2024,
Accepted 9th June 2025

DOI: 10.1039/d4cy01192a

rsc.li/catalysis

Enol ether radical cations are interesting intermediates for various transformations, yet their lifetime can be too short to be harnessed for synthetic organic transformations. An additional methyl group installed in the β-position of an enol ether was found to efficiently control the reactivity, leading to novel electrochemically induced Diels–Alder reactions with enhanced flexibility in view of the substrate structure.

Introduction

Controlling reactive intermediates can lead to the discovery of new modes of bond formation and cleavage.[1] To generate highly reactive species that take part in subsequent transformations, bench-stable substrates can be activated by several means, including thermal, solar, and electrical energy, as well as a wide variety of catalysts. Controlling the reactivity of the short-lived intermediate is a major challenge that must be overcome to achieve the desired synthetic outcome. In this context, organic radical cation species were found to be interesting starting points for various transformations.[2] They offer unique reactivity profiles, in which radical and cation characteristics are merged, enabling otherwise challenging reactions. However, since their lifetime is often too short to be harnessed, creative means are required to use them as intermediates in useful synthetic transformations.

One of the most straightforward ways to generate radical cation species involves an umpolung process *via* single-electron oxidation.[3] Recent advancements in utilizing light[4] and electrical energy[5] have resulted in the development of novel reactions that proceed *via* radical cation intermediates. Frequently used precursors are electron-rich alkenes, sometimes in conjugation with an arene moiety.[6] In this context, we have been developing radical cation reactions by means of photochemical[7] and electrochemical[8] methods in $LiClO_4/CH_3NO_2$ solution (Fig. 1). Mechanistic studies suggest that electro-generated radical cations are particularly well stabilized in this medium.[9] In addition to styrenes (eqn (1)), aryl vinyl ethers (eqn (2)), and enol ethers (eqn (3)) were used as precursors for radical cations as reactive intermediates for cycloadditions (Fig. 1). However, in all these cases, an electron-rich arene moiety, the structural motif we refer to as "redox tag", is required to harness the high reactivity of enol ether radical cations.[10]

Previously, we reported that the reactivity of alkene radical cations is significantly affected by slight changes in the substitution pattern (Fig. 2, eqn (1) and (2)).[11] We thus questioned whether an additional methyl group installed in the β-position could control the reactivity of enol ether radical cations

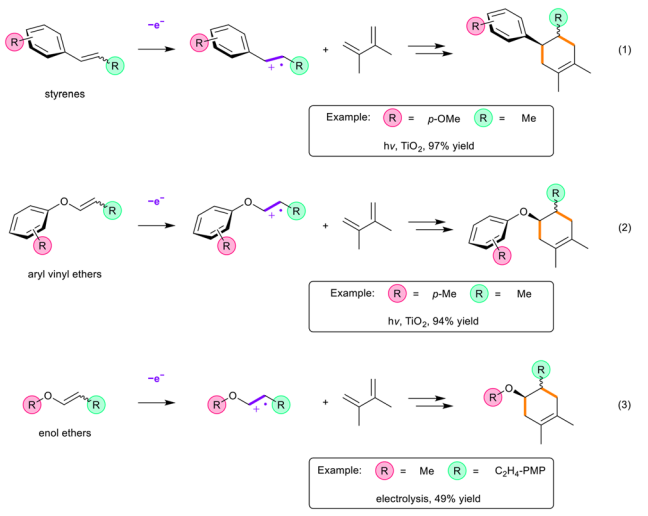

Fig. 1 Previously reported radical cation Diels–Alder-type cycloadditions carried out in $LiClO_4/CH_3NO_2$ solution.[7b,7g,13]

[a] Department of Applied Biological Science, Tokyo University of Agriculture and Technology, 3-5-8 Saiwai-cho, Fuchu, Tokyo 183-8509, Japan. E-mail: yokada@cc.tuat.ac.jp
[b] Leibniz Institute for Catalysis, Albert-Einstein-Str. 29a, 18059 Rostock, Germany. E-mail: robert.francke@catalysis.de
[c] Institute of Chemistry and Department of Life, Light & Matter, University of Rostock, Albert-Einstein-Str. 25 and 27, 18059 Rostock, Germany

† Electronic supplementary information (ESI) available. See DOI: https://doi.org/10.1039/d4cy01192a

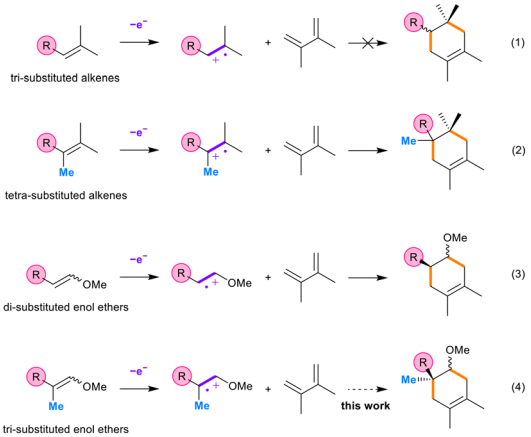

Fig. 2 Effect of an additional methyl group on radical cation [4 + 2] cyclizations.

(eqn (3) and (4)). Described herein is the electrochemically induced Diels–Alder reaction of tri-substituted enol ethers.

Results and discussion

The present work began with the synthesis of tri-substituted enol ether **1** *via* a Wittig reaction of the respective ketone to form the model dienophile for the electrochemically induced Diels–Alder reaction (for details, see the ESI†). The electrolysis of **1** was carried out at a constant potential of 1.2 V *vs.* Ag/AgCl in a 1M $LiClO_4/CH_3NO_2$ electrolyte solution using carbon felt electrodes in the presence of 2,3-dimethyl-1,3-butadiene (**2**) at room temperature. We anticipated that an additional methyl group installed in the β-position would be favorable with respect to the thermodynamic stability of the enol ether radical cation, yet kinetically disfavored in view of subsequent bond formation due to steric hindrance. The reaction proceeded smoothly to give the cycloadduct **3** in good yield even with a catalytic amount of electrical charge, suggesting that backward electron transfer and/or radical cation chain pathways are involved (Table 1, entries 1 and 2).[12] Electrical charge input was found to be essential for the reaction (entry 3), and constant current conditions were also effective (entry 4). Different electrolyte solutions were tested, demonstrating the advantageous properties of $LiClO_4$ and CH_3NO_2 as supporting electrolyte and solvent, respectively (entries 5 and 6).

To our surprise, enol ether **4**, which carries no activating aryl substituent, was also found suitable for [4 + 2] cycloaddition (Scheme 1, eqn (1)). This is clearly different from our previous observations using the di-substituted enol ether **6**, where a methoxy group installed in the *para* position of the arene was essential for successful conversion (eqn (2)).[13]

With these results in hand, a mechanistic picture can now be drawn for the reactions of the enol ethers (Fig. 3). First, anodic oxidation leads to the formation of radical cations, which spontaneously undergo [4 + 2] cyclization with the diene. In the cases of the di-substituted enol ether substrates

Table 1 Control experiments for the electrochemically induced Diels–Alder reaction of **1**

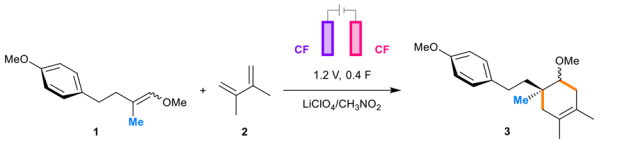

Entry	Deviation from standard conditions[a]	Yield (%)[b]
1	None	91[c] (0)
2	1.0F	81 (0)
3	No electricity	0 (99)
4	0.5 mA	85 (0)
5	$^nBu_4NClO_4$ instead of $LiClO_4$	40 (36)
6	CH_3CN instead of CH_3NO_2	70 (0)

[a] All reactions were carried out on a 0.20 mmol scale with respect to the enol ether **1**, in the presence of 2 equiv. 2,3-dimethyl-1,3-butadiene (**2**) in 1M $LiClO_4/CH_3NO_2$ (20 mL) using an undivided cell under Ar at rt. [b] Yields were determined by ^1H NMR analysis using benzaldehyde as an internal standard. ^1H NMR yields of unreacted starting material are reported in parentheses. [c] Isolated yield.

6 and **7**, positive charge and spin density are accommodated by the redox tag, whereas a relatively stable cyclohexene radical cation is obtained upon conversion of tri-substituted enol ethers **1** and **4**. After cycloaddition, the positive charge is passed to another substrate molecule (chain process) or returned to the anode (backward electron transfer), resulting in sub-stoichiometric charge consumption. Using cyclic voltammetry, it was confirmed that the redox potential of the product is more positive than the redox potential of the substrate (see the ESI†), a precondition for both the chain process and the backward electron transfer.[15]

The triggering of redox-neutral conversions by electric charge observed herein has been used occasionally in other applications (*e.g.*, molecular rearrangements and ArSN reactions). The corresponding reactions have been named as "electrocatalyzed"[14] or "electrochemically catalyzed".[15] In the present case, it appears plausible that the additional methyl group installed in the β-position of the enol ether stabilizes the cyclohexene radical cation and thus eliminates the need for stabilization by redox tags.

To probe the mechanisms shown in Fig. 3, quantum chemical calculations were performed. Geometry optimization of all intermediates was carried out at the ωB97X-D3 level of theory[16] with the def2-TZVP basis set[17] using the CPCM model to account for solvent effects.[18] All Gibbs free energies calculated for substrates, intermediates, and products are summarized in the ESI.† Two pathways were calculated starting from the *E*- and the *Z*-forms of the enol ethers, leading to the *trans*- and the *cis*-products, respectively.‡ The energies of the *E*-enol ether substrates **4**, **6**,

‡ A possible rotation around the C_α–C_β bond of the enol ether radical cations and thus a cross over between the *E*- and *Z*-pathways was not considered in this study. This aspect, together with a more detailed investigation of the cycloaddition step (including activation barriers), is subject of ongoing work.

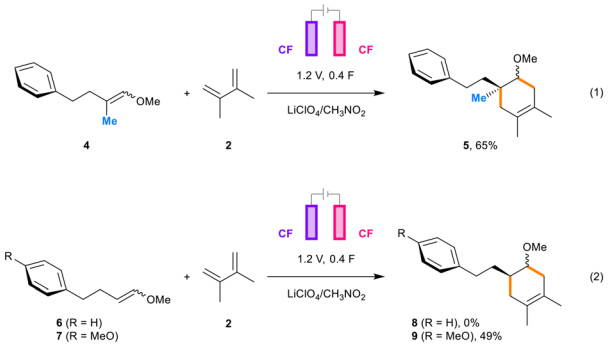

Scheme 1 Electrochemically induced Diels–Alder reactions of enol ethers.

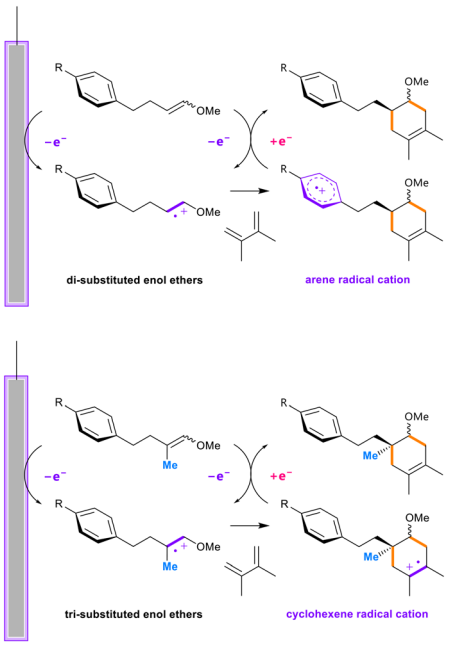

Fig. 3 Plausible mechanisms that explain the different reactivity profiles of di- and tri-substituted enol ethers.

and **7** were found to be 0.16, 0.02, and 0.16 kcal mol^{-1} lower than the corresponding *Z*-configurations, respectively. The profiles are shown exemplary for the *E*-pathway, while the profiles for the *Z*-pathway are summarized in Fig. S2.†

The calculations demonstrate that the cycloaddition step is thermodynamically favorable along all computed pathways. The relative Gibbs free energies suggest that in the reactions of **4** and **7**, the final reduction step releases more energy than is consumed by the initial oxidation step ($|\Delta G^0_{red}| > |\Delta G^0_{ox}|$, see Table 2), which is a prerequisite for a spontaneous chain process or a backward electron transfer as mentioned before.[15] In contrast, for substrate **6**, the opposite trend is observed ($|\Delta G^0_{red}| < |\Delta G^0_{ox}|$). This computational finding aligns with experimental results, where products **5** and **9** are obtained in 65% and 49% yield, respectively, whereas product **8** is not formed (0% yield). A closer look at the energy profiles reveals that the β-methyl group in **4** causes a

Table 2 Redox energy gaps ($|\Delta G^0_{ox}| - |\Delta G^0_{red}|$) for the studied radical cation [4 + 2] cyclizations

Substrate	Product	Redox energy gap [kcal mol^{-1}]
E-**4**	*trans*-**5**	−4.04
Z-**4**	*cis*-**5**	−5.23
E-**6**	*trans*-**8**	1.96
Z-**6**	*cis*-**8**	1.64
E-**7**	*trans*-**9**	−0.22
Z-**7**	*cis*-**9**	−1.55

particularly strong stabilization of the corresponding radical cation and thereby smaller ΔG^0_{ox} values compared to **6** and **7**. This results in a more pronounced redox energy gap ($|\Delta G^0_{ox}| < |\Delta G^0_{red}|$, see Table 2), which is equivalent to additional driving force for the chain process and backward electron transfer, respectively.

To understand the role of aromatic moieties during the transformations, it is worth comparing the spin density maps of intermediates $\mathbf{5}^{\bullet+}$, $\mathbf{8}^{\bullet+}$ and $\mathbf{9}^{\bullet+}$. In line with the plausible mechanism in Fig. 2, all configurations of $\mathbf{5}^{\bullet+}$ and $\mathbf{8}^{\bullet+}$ display a spin density that is primarily localized in the C=C double-bonded region of the cyclohexene moiety (see exemplary for *trans*-$\mathbf{5}^{\bullet+}$ in Fig. 4B – all spin density plots are shown in Fig. S3†). Although both substrates contain an aryl group, which could potentially contribute to electron delocalization, the relatively low spin density observed on the benzene ring

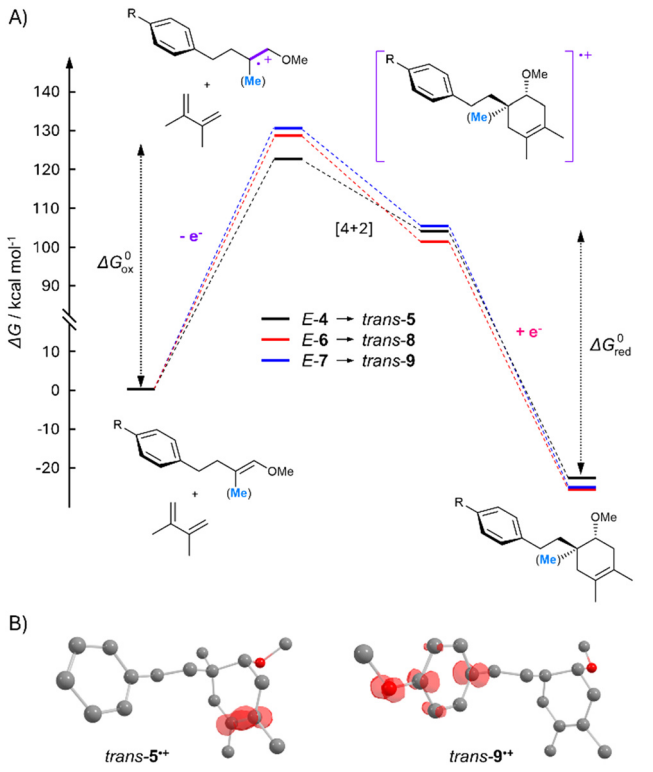

Fig. 4 A) Gibbs free energy profile for the conversion of the *E*-enol ethers **4**, **6**, and **7**. B) Spin density distributions for the *trans* configurations of radical cations of $\mathbf{5}^{\bullet+}$ and $\mathbf{9}^{\bullet+}$ (contour value = 0.016).

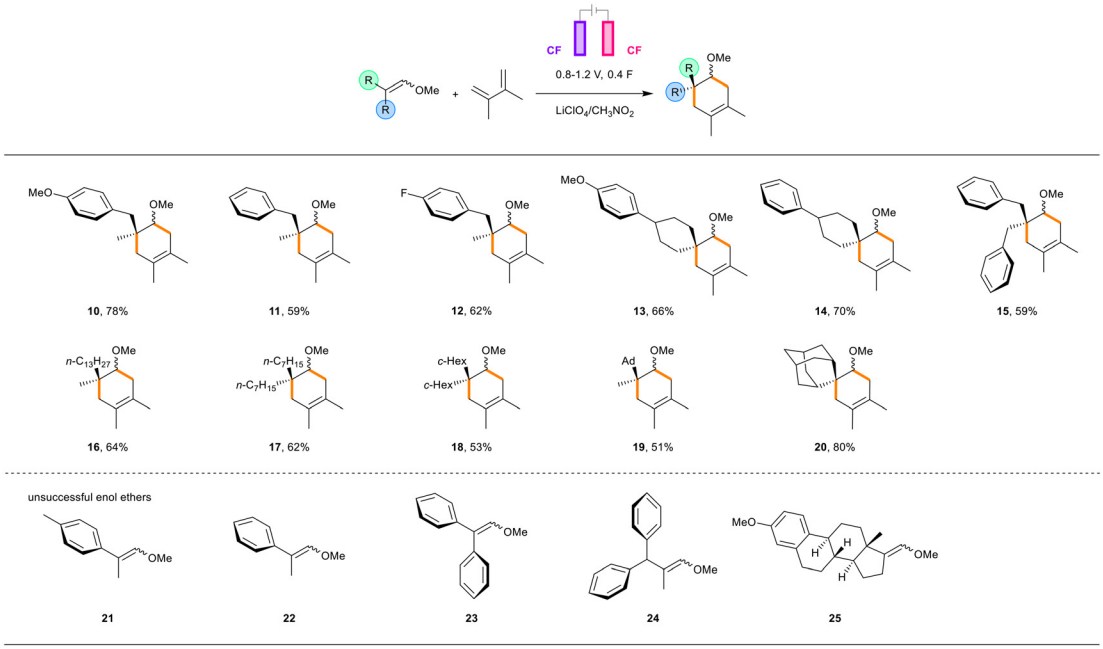

Scheme 2 Scope of the electrochemically induced Diels–Alder reaction. The standard conditions of Table 1 were applied, whereby the working electrode potential was adapted to the individual substrates (for details see the ESI†).

suggests that its stabilizing effect on the cycloadduct radical cation is negligible. However, in $\mathbf{9}^{\bullet+}$, the presence of a strongly electron-donating methoxy group facilitates spin density delocalization onto the aromatic ring (Fig. 4B and S3†), indicating that the latter plays a crucial role in the conversion of **7** → **9**.

We anticipated that the advantageous impact of the β-methyl group would significantly broaden the scope of the reaction, since an electron-rich arene moiety, the "redox tag", is not required. Indeed, a wide variety of tri-substituted enol ethers was successfully converted under the standard conditions (Scheme 2). Both arene-containing **10–15** and arene-free **16–20** enol ethers were compatible with the protocol, including substrates **18–20** that carry one or two sterically demanding tertiary β-alkyl groups. However, conversion of enol ethers that are directly conjugated with aryl substituents **21–23** was not successful, suggesting that the reactivity of the resulting styrene radical cations was different. Furthermore, the diphenyl methyl group **24** was incompatible with the method, probably due to the easily oxidizable benzylic position. Electrolysis of the estrone-derived enol ether **25** was also unproductive.

Conclusions

In conclusion, we have demonstrated that an additional methyl group installed in the β-position of an enol ether can control its radical cation reactivity, leading to the development of novel electrochemically induced Diels–Alder reactions with a broad scope. The results presented herein highlight the unique reactivity of tri-substituted enol ether radical cations, enabling electrochemically induced [4 + 2] cyclizations of redox tag-free substrates, thereby upgrading their synthetic utility as reactive intermediates. A plausible explanation for the observed behavior is that the additional β-substituent enhances the stability of the enol ether radical cation, which was confirmed by quantum chemical calculations. These calculations also show that the redox energy for the oxidation step becomes smaller relative to the one for reduction ($|\Delta G^0_{red}| > |\Delta G^0_{ox}|$), resulting in additional driving force for the radical cation chain process/backward electron transfer. Although our computational results provide essential insights into the reaction mechanism, more detailed calculations in combination with further experiments are required for a comprehensive understanding. A mechanistic study on electrochemically induced Diels–Alder reactions of trisubstituted enol ethers is underway in our laboratory.

Data availability

The data supporting this article have been included as part of the ESI.†

Conflicts of interest

There are no conflicts to declare.

Acknowledgements

This work was supported in part by JSPS KAKENHI Grant Numbers 22K05450 (to Y. O.), 23KJ0870 (to H. M.), TEPCO Memorial Foundation (to Y. O.), and JST COI-NEXT Grant Number JPMJPF2104 (to Y. O.). The authors are also grateful for financial support through the DFG Heisenberg Program

(FR 3848/4-1, to R. F.), the Chinese Scholarship Council (PhD stipend, to Y. H.), the DFG RTG SPECTRE (no. 507189291, to O. S. B.), and the Leibniz Association through the Leibniz Competition (to O. S. B.). The authors thank FORTE Science Communications for English language editing.

Notes and references

1 M. S. Singh, *Reactive Intermediates in Organic Chemistry: Structure, Mechanism, and Reaction*, Wiley-VCH, Weinheim, 2014.
2 For selected reviews, see: (*a*) H.-M. Huang, M. H. Garduño-Castro, C. Morrill and D. J. Procter, *Chem. Soc. Rev.*, 2019, **48**, 4626; (*b*) J. K. Matsui, S. B. Lang, D. R. Heitz and G. A. Molander, *ACS Catal.*, 2017, **7**, 2563; (*c*) M. Yan, J. C. Lo, J. T. Edwards and P. S. Baran, *J. Am. Chem. Soc.*, 2016, **138**, 12692; (*d*) S. W. M. Crossley, C. Obradors, R. M. Martinez and R. A. Shenvi, *Chem. Rev.*, 2016, **116**, 8912; (*e*) R. W. Hoffmann, *Chem. Soc. Rev.*, 2016, **45**, 577; (*f*) Z.-M. Chen, X.-M. Zhang and Y.-Q. Tu, *Chem. Soc. Rev.*, 2015, **44**, 5220; (*g*) B. Zhang and A. Studer, *Chem. Soc. Rev.*, 2015, **44**, 3505; (*h*) S. Tang, K. Liu, C. Liu and A. Lei, *Chem. Soc. Rev.*, 2015, **44**, 1070; (*i*) U. Wille, *Chem. Rev.*, 2013, **113**, 813.
3 R. D. Little and K. D. Moeller, *Electrochem. Soc. Interface*, 2002, **11**, 36.
4 For selected reviews, see: (*a*) M. Silvi and P. Melchiorre, *Nature*, 2018, **554**, 41; (*b*) J. Twilton, C. Le, P. Zhang, M. H. Shaw, R. W. Evans and D. W. C. MacMillan, *Nat. Rev. Chem.*, 2017, **1**, 0052; (*c*) N. A. Romero and D. A. Nicewicz, *Chem. Rev.*, 2016, **116**, 10075; (*d*) K. L. Skubi, T. R. Blum and T. P. Yoon, *Chem. Rev.*, 2016, **116**, 10035; (*e*) M. D. Kärkäs, J. A. Porco, Jr. and C. R. J. Stephenson, *Chem. Rev.*, 2016, **116**, 9683; (*f*) C. K. Prier, D. A. Rankic and D. W. C. MacMillan, *Chem. Rev.*, 2013, **113**, 5322.
5 For selected reviews, see: (*a*) M. Rafiee, M. N. Mayer, B. T. Punchihewa and M. R. Mumau, *J. Org. Chem.*, 2021, **86**, 15866; (*b*) R. D. Little, *J. Org. Chem.*, 2020, **85**, 13375; (*c*) M. D. Kärkäs, *Chem. Soc. Rev.*, 2018, **47**, 5786; (*d*) S. Möhle, M. Zirbes, E. Rodrigo, T. Gieshoff, A. Wiebe and S. R. Waldvogel, *Angew. Chem., Int. Ed.*, 2018, **57**, 6018; (*e*) A. Wiebe, T. Gieshoff, S. Möhle, E. Rodrigo, M. Zirbes and S. R. Waldvogel, *Angew. Chem., Int. Ed.*, 2018, **57**, 5594; (*f*) S. R. Waldvogel, S. Lips, M. Selt, B. Riehl and C. J. Kampf, *Chem. Rev.*, 2018, **118**, 6706; (*g*) K. D. Moeller, *Chem. Rev.*, 2018, **118**, 4817; (*h*) J. E. Nutting, M. Rafiee and S. S. Stahl, *Chem. Rev.*, 2018, **118**, 4834; (*i*) J. Yoshida, A. Shimizu and R. Hayashi, *Chem. Rev.*, 2018, **118**, 4702; (*j*) Y. Jiang, K. Xu and C. Zeng, *Chem. Rev.*, 2018, **118**, 4485; (*k*) M. Yan, Y. Kawamata and P. S. Baran, *Chem. Rev.*, 2017, **117**, 13230.
6 K. D. Moeller, *Tetrahedron*, 2000, **56**, 9527.
7 For recent examples, see: (*a*) S. Adachi, N. Maeta, K. Nakayama, Z. Wang, Y. Hashimoto and Y. Okada, *Synthesis*, 2023, **55**, 3013; (*b*) S. Adachi, G. Horiguchi, H. Kamiya and Y. Okada, *Eur. J. Org. Chem.*, 2022, e202201207; (*c*) Y. Hashimoto, G. Horiguchi, H. Kamiya and Y. Okada, *Chem. – Eur. J.*, 2022, **28**, e202202018; (*d*) K. Nakayama, H. Kamiya and Y. Okada, *Beilstein J. Org. Chem.*, 2022, **18**, 1100; (*e*) N. Maeta, H. Kamiya and Y. Okada, *J. Org. Chem.*, 2020, **85**, 6551; (*f*) N. Maeta, H. Kamiya and Y. Okada, *Org. Lett.*, 2019, **21**, 8519; (*g*) K. Nakayama, N. Maeta, G. Horiguchi, H. Kamiya and Y. Okada, *Org. Lett.*, 2019, **21**, 2246.
8 For recent examples, see: (*a*) G. Horiguchi and Y. Okada, *Eur. J. Org. Chem.*, 2022, e202201022; (*b*) S. Tanami, S. R. Hussaini, Y. Kitano, K. Chiba and Y. Okada, *Eur. J. Org. Chem.*, 2022, e202201023; (*c*) Y. Okada, Y. Yamaguchi and K. Chiba, *ChemElectroChem*, 2019, **6**, 4165.
9 (*a*) Y. Okada, *Chem. Rec.*, 2021, **21**, 2223; (*b*) Y. Okada, *Electrochemistry*, 2020, **88**, 497; (*c*) N. Shida, Y. Imada, Y. Okada and K. Chiba, *Eur. J. Org. Chem.*, 2020, 570; (*d*) Y. Imada, Y. Yamaguchi, N. Shida, Y. Okada and K. Chiba, *Chem. Commun.*, 2017, **53**, 3960.
10 (*a*) Y. Okada and K. Chiba, *Chem. Rev.*, 2018, **118**, 4592; (*b*) Y. Okada, *J. Org. Chem.*, 2019, **84**, 1882; (*c*) Y. Okada, A. Nishimoto, R. Akaba and K. Chiba, *J. Org. Chem.*, 2011, **76**, 3470.
11 A. Ozaki, Y. Yamaguchi, Y. Okada and K. Chiba, *Chin. J. Chem.*, 2019, **37**, 561.
12 (*a*) A. F. Roesel, M. Ugandi, N. T. T. Huyen, M. Májek, T. Broese, M. Roemelt and R. Francke, *J. Org. Chem.*, 2020, **85**, 8029; (*b*) K. Nakayama, H. Kamiya and Y. Okada, *J. Electrochem. Soc.*, 2020, **167**, 155518; (*c*) Y. Okada, R. Akaba and K. Chiba, *Tetrahedron Lett.*, 2009, **50**, 5413.
13 H. Morizumi, K. Nakayama, Y. Kitano and Y. Okada, *Synlett*, 2024, **35**, 362.
14 (*a*) Y. Imada, Y. Okada and K. Chiba, *Beilstein J. Org. Chem.*, 2018, **14**, 642; (*b*) K. Chiba, T. Miura, S. Kim, Y. Kitano and M. Tada, *J. Am. Chem. Soc.*, 2001, **123**, 11314; (*c*) Y. Okada, Y. Yamaguchi, A. Ozaki and K. Chiba, *Chem. Sci.*, 2016, **7**, 6387; (*d*) T. Yamamoto, B. Riehl, K. Naba, K. Nakahara, A. Wiebe, T. Saitoh, S. R. Waldvogel and Y. Einaga, *Chem. Commun.*, 2018, **54**, 2771; (*e*) T. Broese, A. F. Roesel, A. Prudlik and R. Francke, *Org. Lett.*, 2018, **20**, 7483.
15 (*a*) R. Francke and R. D. Little, *Curr. Opin. Electrochem.*, 2023, **40**, 101315; (*b*) R. Francke and R. D. Little, *ChemElectroChem*, 2019, **6**, 4373; (*c*) C. Costentin and J.-M. Savéant, *Proc. Natl. Acad. Sci. U. S. A.*, 2019, **116**, 11147.
16 (*a*) J.-D. Chai and M. Head-Gordon, *Phys. Chem. Chem. Phys.*, 2008, **10**, 6615; (*b*) S. Grimme, J. Antony, S. Ehrlich and H. Krieg, *J. Chem. Phys.*, 2010, **132**, 154104.
17 V. Barone and M. Cossi, *J. Phys. Chem. A*, 1998, **102**, 1995.
18 (*a*) M. Cossi, N. Rega, G. Scalmani and V. Barone, *J. Comput. Chem.*, 2003, **24**, 669; (*b*) M. Cossi, N. Rega, G. Scalmani and V. Barone, *J. Comput. Chem.*, 2003, **24**, 669.